

Local Drag Reduction Due to Injection of Polymer Solutions into Turbulent Flow in a Pipe

Part I: Dependence on Local Polymer Concentration

W. D. McCOMB and L. H. RABIE

School of Engineering
University of Edinburgh
Edinburgh, Scotland

Aqueous solutions of drag-reducing polymers were injected into turbulent water flow in a pipe. The injection point was situated where the flow was well-developed. Thus, subsequent streamwise variations in pressure drop were due to the injected polymer spreading out across the pipe. The axial development of local drag reduction was monitored by a series of closely-spaced pressure tapings. The corresponding radial dispersion of the injected polymer, as it travelled downstream, was assessed by sampling the flow at various points.

Local drag reduction, due to either point injection at the centerline or injection through a slot in the wall, was found to increase with distance downstream. This increase was related to the streamline increase of polymer concentration in a narrow annulus near the pipe wall. It was tentatively concluded that the effective annulus was bounded by $15 \leq y^+ \leq 100$, in agreement with previous deductions from less direct evidence.

SCOPE

The enhanced mixing due to turbulence makes the use of turbulent flows very attractive in many industrial processes. For instance, in pipe flows, the large rates of heat or mass transfer in the radial direction are crucial to many applications. Unfortunately, the correspondingly high rate of momentum transfer in the radial direction leads to a large dissipation of energy, with a consequent penalty in pumping costs. Evidently, methods of reducing this energy dissipation (or drag) are of some interest.

The use of polymer additives to reduce drag has received a great deal of attention in recent years and there are now some extensive reviews of the subject (e.g., Hoyt, 1972, 1977; Little et al., 1975; Virk, 1975). Even only a few parts per million of high molecular weight additives can reduce drag by amounts up to about 80%. Thus, the technique is potentially very important.

However, there are also some disadvantages in the use of these additives. They degrade under shear and lose their effectiveness; their cost may be prohibitive; and their presence may be undesirable in some parts of the flow system. While more resistant (or even "self-healing") additives may be developed, an alternative approach would be to devise some modification to the boundary surface which would reproduce the effect of the polymers on the turbulence. Such a modification would be a permanent effect and need only be used in those parts of the system where a reduction in drag was required.

Any hope of developing drag-reducing surfaces in this way must rest on our possessing a detailed picture of the way the dissolved polymers modify the turbulence. Although there has been a great deal of research on drag reduction, relatively little

attention has been given to the polymer-turbulence interaction. In particular, although it is widely assumed that the polymers act in the vicinity of the pipe wall, this is generally inferred *indirectly* from (for example) measurements of velocity distributions. The only *direct* demonstration that the polymer molecules must be present in the wall region for there to be drag reduction was an investigation by Wells and Spangler (1967). These authors injected polymer solution at the wall of a pipeflow and found that wall shear stress was reduced immediately. Whereas when polymer was injected into the turbulent core, no effect was observed until the polymer had diffused to the wall region.

The objective of the present work was to carry out a similar, but much more quantitative, investigation. To begin with, we used many closely-spaced pressure tapings to monitor the axial pressure development, downstream from the injection point. Thus, as the injected polymer spread out radially (as it was carried downstream), we could observe the decrease in axial pressure drop as the polymer concentration increased in the wall region. Then, in order to measure the polymer concentration, salt was added to the injected solutions and samples were taken over a radial traverse at a series of stations downstream from the injector. Thus, we could seek to answer the question: What is the relationship between the amount of drag reduction (at a particular point downstream from the injector) and the amount of polymer in any given annulus at the same downstream distance? From this, we could hope to identify the precise region where the polymer molecules interacted with the local fluid turbulence.

CONCLUSIONS AND SIGNIFICANCE

1. When polymer solution was injected at the centerline of the pipe, the *local* drag reduction increased with distance

downstream from the injection point. This was due to the polymer spreading out radially, as the injected solution was carried downstream. When the polymer solution was spread uniformly across the pipe, the local drag reduction attained its constant, asymptotic value.

Correspondence concerning this paper should be addressed to W. D. McComb. L. H. Rabie is now at Mechanical Engineering Department, Mansoura University, Egypt.
0001-1541-82-6094-0547-\$2.00. © The American Institute of Chemical Engineers, 1982.

2. When polymer solution was injected at the wall of the pipe, the local drag reduction again increased with distance downstream, but at a more rapid rate than when injection was at the centerline. Also, the variation of drag reduction with downstream distance tended to show a slight overshoot before falling off to the same asymptotic level as in centerline injection.

3. From the above two points we may conclude that the polymer molecules interact with the turbulence in an annulus which is *near* but not *at* the wall. More quantitatively, the streamwise increase in local drag reduction was related to the streamwise increase of polymer concentration in a narrow annulus near the pipe wall. A close correlation of the two was achieved for an annulus centered at $0.9 R$ and with an overall radial thickness of $0.15 R$, where R was the pipe radius. In wall region coordinates, this corresponds to an annulus bounded by $15 \leq y^+ \leq 100$. These results were obtained for two different polymers (polyethyleneoxide and polyacrylamide) and two different master solution concentrations.

4. For both types of injection, the asymptotic drag reduction

was greater than that obtained with homogeneous solutions under otherwise identical conditions. This was particularly noticeable at lower Reynolds numbers. It was attributed to a reduced onset wall shear stress, probably due to the presence of molecular aggregates, rather than individual molecules.

5. For injection at the wall, the streamwise curves of local drag reduction were found to have an oscillatory scatter of the data points.

These oscillations were attributed to the quasi-cyclic variations in the turbulent bursting process. (In recent years, it has been found that turbulence production in shear flows is intermittent. Turbulence is generated in the boundary layer during periods of activity which are known as bursts.) It was argued that the rate at which polymer solution would reach the buffer region from the wall (or leave the buffer region for the core) would be intermittent from this cause. A calculation of the time between bursts on this basis was later confirmed by an independent measurement obtained using laser anemometry.

REVIEW OF RELATED WORK

As part of a general study of turbulent drag reduction and other non-Newtonian fluid motion (e.g., McComb and Chan, 1979; McComb and Ayyash, 1980; the second of these contains a number of other references), we have observed the effect of injecting concentrated solutions of drag-reducing polymers into turbulent flow. Our aim has been to produce a developing situation in which the local drag reduction at a given section would depend on the radial distribution of the dissolved polymers over that section. Hence, we could hope to learn something about local polymer—turbulence interactions.

Before discussing related work, we should perhaps make two points. First, most work on drag reduction by additives has involved the use of pre-mixed solutions (or suspensions) of the additive. In such solutions, the additives may be assumed to be uniformly distributed throughout the flow (although, of course, there may be local inhomogeneities such as aggregates). As the general subject is well covered by the reviews already cited, we shall confine our attention here to experiments where polymer solutions were injected into the bulk flow of the solvent.

Our second point is concerned with the fact that injection techniques have generally been employed mainly as a practical expedient, where premixing of the polymer would be either uneconomic or otherwise undesirable. Not surprisingly, most reports in this area deal with external flows over a solid body (e.g., Love, 1965; Johnson and Barchi, 1968; Granville, 1969; Latto and Shen, 1970; Wu, 1971; Kowalski and Brundrett, 1974), but some practical studies have also been made using boundary—layer or wall—region injection in pipe flows (e.g., Goren and Norbury, 1967; Maus and Wilhelm, 1970; Walters and Wells, 1971; Ramu and Tullis, 1976). While these papers, in the main, tend to deal with practical aspects of optimizing drag reduction, several of their conclusions are of more general interest and we shall return to these at a later stage. However, this brings us to our second point. As in the papers just cited, the amount of drag reduction (or the way in which it varies) may well depend on the parameters of the injection process. In particular, for injection at the wall, factors like injection angle or slot width may well be important, from a practical point of view. But that is not the objective of the present work.

What we aim to do is to produce a developing situation in which we can try to establish a relationship between the streamwise variation of local drag reduction and the radial variation of polymer concentration. Any injector which produces such a situation will be adequate to our purpose. The trial of different injectors to produce different concentration distributions (and hence different drag reductions) is quite another problem and will not be considered here.

Let us turn now to the use of injection techniques as a means of understanding drag reduction. Apparently, the only attempt to show *directly* that the presence of the polymer in the wall region is crucial to drag reduction was an investigation by Wells and Spangler (1967). It was found that when polymer was introduced into the wall region of a turbulent pipe flow, the wall shear stress was reduced immediately downstream from the injection point. Whereas, when the polymer was injected into the turbulent core, no effect was observed until the polymer had diffused to the wall region. In view of the somewhat incomplete nature of the investigation, it amounts to a direct, but only qualitative, demonstration of this point.

Later use of injection techniques has produced contradictory results. Vleggaar and Tels (1973) injected a concentrated polymer solution into the core region of a turbulent pipe flow. Their results indicated that substantial drag reduction occurred before the polymer reached the wall region. The drag reduction effect was larger than in premixed polymer solutions of equivalent concentration (i.e., "homogeneous drag reduction," according to the authors) and characterized by the lack of an onset shear stress. Their flow visualization showed that the injected polymer formed a long thread which resisted dispersion and extended downstream for a distance of more than 200 tube diameters. They concluded that the polymer thread interacted with the eddies in the core region to produce a new type of drag reduction.

Stenberg et al. (1977a, 1977b) also injected concentrated polymer solutions into pipe flow, but in their apparatus the injection was at the inlet of the pipe, via a rotating impeller mixer. Pressure drops were measured when the mixer was inoperative and also when it was running at various speeds. With no mixing or poor mixing, their results were in agreement with those of Vleggaar and Tels and showed reduced onset stress (also compare Goren and Norbury, 1967). However, with efficient mixing, the usual behavior of homogeneous solutions was regained. Dye visualization and Schlieren photographic studies revealed the presence of small visible polymer strands which disappeared when the mixer was used. Stenberg et al. concluded from their results that there was no essential difference between homogeneous and heterogeneous forms of drag reduction. But, the question of where the polymers act in the two cases was not considered.

Finally, we have ourselves reported some preliminary results of the present work (McComb and Rabie, 1978a, 1978b).

EXPERIMENTAL APPARATUS

The apparatus consisted of an open-circuit water flow rig; a polymer injection system; a sampling system to measure local

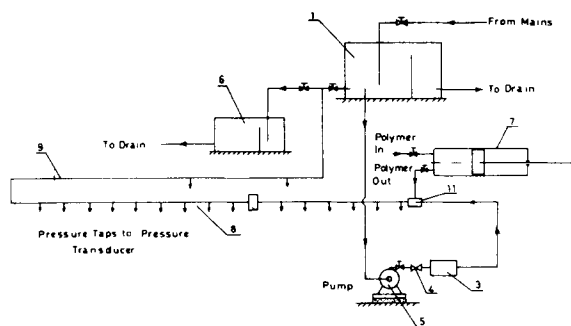


Figure 1. Flow diagram of the experimental apparatus: (1) supply tank; (2) rigid PVC pipe section; (3) settling chamber; (4) orifice meter; (5) pump; (6) constant-level overflow tank; (7) injection pump; (8) first pass of the test section; (9) second pass of the test section; (10) scanning valves; and (11) polymer injector.

polymer concentrations in the flow; and an LDA setup. Details of the latter item will be given in a subsequent paper (Part II).

Water Flow Rig

A schematic flow diagram is provided in Figure 1. As Figure 1 shows, water was supplied to a constant head overflow tank from the laboratory main supply. The water was then pumped from the header tank to the test section through a settling chamber and entrance length. The first part of the test section was fitted with a larger number of pressure taps to monitor the development of drag reduction in the flow direction. After a U-bend, the return leg (or second pass) had a pair of pressure taps to act as a control. The open-circuit arrangement was used throughout.

The working section was made from Perspex (acrylic) pipe of 26 mm ID. The first pass was 6 m long and was connected by a U-bend to the second pass of 4 m in length, both pipes being parallel and horizontal. (The level of the second pass was 0.1 m higher than the first, to allow for later use of LDA.) The polymer injector was fixed between flanges at the entrance of the first pass.

The first pass was fitted with 18 pressure taps, the first of these being located 0.05 m downstream from the injector position. This was followed at 0.3 m by a series of ten taps equispaced at 0.3 m intervals and then a further seven taps at 0.4 m intervals. The two pressure taps in the second pass were separated by 1.0 m. The pressure taps could be connected in turn through a rotary switch valve to a DISA low-pressure transducer (model 51 D20). This was of the capacitive type and a set of ten diaphragms permitted its use from a lowest range of 0.03 m water head to a highest range of 196 m water head. The transducer was calibrated using a static pressure head and the calibration was checked at intervals.

The flow rate of the water in the system was measured using a calibrated orifice meter. This was fitted to the system just downstream from the pump. The pressure difference across the orifice was also measured on the pressure transducer.

Polymer Injection System

The pump used to inject the polymer solutions consisted of a piston sliding in a cylinder. Efficient sealing ensured that the injection flow rate was entirely governed by the rate of piston travel. This, in turn, was controlled by the rotation of a threaded rod driven through a reduction gear by an electric motor. The injection flow rates were in the range 1.0 to 18.0 mL/s. As the capacity of the pump was 15 L, this meant that the shortest injection stroke lasted at least 15 minutes. This was long enough to perform all necessary measurements in one run without having to recharge the pump.

The centerline injector had to be small enough to disturb the pipe flow as little as possible; yet large enough to ensure low shear stresses in the injection flow (i.e., to minimize polymer degradation). It was made of 2.3 mm ID \times 3.00 mm OD stainless steel tube, bent through 90° to deliver the polymer solution in the direction of the water flow. The length in the flow direction was 30 mm and an

upstream fairing 25 mm long was used in order to reduce flow disturbance.

The wall injector was of the slot type. It consisted of two Perspex rings, machined such that an internal circumferential gap was formed when they were assembled together. The two rings were separated by a paper gasket; varying the gasket thickness determined the width of the slot. Some preliminary tests were made to choose a slot width which gave a satisfactory rate of development (i.e., the drag reduction did not develop too rapidly). A slot width of 4 mm in the flow direction was found to be satisfactory. The inner diameter of the injector was 26 mm, to match the pipe diameter. The slot was inclined at an angle of 8° to the flow direction which allowed the polymer to be introduced as near tangentially to the flow as possible.

Sampling System

The system used to withdraw samples if the fluid consisted of a Perspex ring (which was mounted between flanges in the pipe test section); a sampling tube assembly; and a micrometer traverse. The inside diameter of the Perspex ring was 0.8 mm larger than the pipe diameter to allow for the size of the sampling tube and permit flow samples to be taken near the wall.

The sampling tube was a hypodermic needle bent through 90° to face the flow. Its dimensions were 0.5 mm ID \times 0.8 mm OD \times 10 mm long in the flow direction. This was mounted on a stainless steel tube of 0.85 mm ID \times 1.2 mm OD which in turn was attached to the micrometer traverse so that samples could be taken at any radial position. The outlet of the sampling system was fitted with a valve to control the sampling flow rate.

During the concentration measurements only, the 6 m long first pass of the test section was replaced by a similar pipe, divided into six sections (rather than two) by flanged joints. The six sections were 2.0 m, 2.0 m, 1.0 m, 0.5 m, 0.25 m and 0.25 m long, and the sampling system could be inserted between the flanges at any of these joints. The electrical conductivity of the collected samples was measured using a conductivity cell connected to a direct-reading conductivity meter (Portland Electronics Series 300 Model P335). The meter had a compensator to take account of temperature difference effects on the conductivity measurements.

Further details of the construction of the apparatus; the calibration procedures; and the results of the calibration will be found in the thesis by Rabie (1978).

EXPERIMENTAL PROCEDURE

Pressure-Drop and Concentration Measurements

The water flow rate Q_w was set to give the required Reynolds number and this value was monitored throughout the experiment using the orifice flowmeter. The water temperature was checked at frequent intervals during each experiment.

Streamwise pressure drops were measured relative to the reference tapping by using the rotary switch valves to select each pressure tapping as required. The pressure drops were measured on the capacitive-type transducers and output as voltages to the data-logging system. For each pair of taps, ten values were processed on the computer to give mean values of pressure drop (and friction factor) appropriate to the mid-point of each pair of pressure tappings. In all cases, the output of the transducer was smoothed electronically with a 1.0 second time period before being fed to the data logger.

Polymer solutions were injected using the piston-in-cylinder arrangement at either the centerline or wall injector. The injection flow rate of the polymer solution Q_p was measured by timing the displacement of the piston during the experiment. After the injection flow was established, the water flow was adjusted to keep Q_w at the value before polymer injection. Pressure drops were again measured, as described above, and used to calculate the local reduction in friction as a function of distance downstream from the injector.

To measure the radial distribution of the polymers, samples were withdrawn from the flow at various radial positions and at various downstream distances. The solutions used, contained salt (NaCl) to act as a tracer. The salt concentration of each sample was determined by measuring its electrical conductivity. It was assumed that the concentration of polymer in the samples (relative to the initial value) was proportional to the relative concentration of salt. The validity of this assumption will be discussed later, in the light of the results obtained.

Full details of the sampling procedure may be found elsewhere (Rabie, 1978), but two precautions taken are worthy of mention here. First, when the sampling tube was positioned at the required radius, residual fluid from the previous sample was allowed to bleed away. Second, the sampling flow rate was adjusted to ensure that only liquid from the immediate neighborhood of the sample tube tip would be withdrawn.

Data Analysis

The apparatus was designed to give well-developed turbulent flow in the test section. Let us begin by listing some of the basic definitions. The pressure gradient was obtained from the slope of the streamwise pressure variation and the wall shear stress and friction velocity calculated in the usual way, thus:

$$\tau_w = \frac{d}{4} \frac{dp}{dx} \quad (1)$$

and

$$u^* = \sqrt{\frac{\tau_w}{\rho}} \quad (2)$$

The friction factor and Reynolds number were calculated from

$$f = 2(u^*/\bar{U}_{av}) \quad (3)$$

and

$$Re = \bar{U}_{av} d / \nu, \quad (4)$$

where the bulk mean velocity is obtained from

$$\bar{U}_{av} = 4Q_w / \pi d^2. \quad (5)$$

With the injection of polymer, the local drag reduction was defined in terms of ΔP_p and ΔP_w , the pressure drops across a pair of taps with, and without, polymer injection, respectively. Hence, the local drag percentage reduction was calculated for the midpoint of a given pair of taps as

$$DR = \frac{(\Delta P_w - \Delta P_p)}{\Delta P_w} \times 100\%. \quad (6)$$

In most drag reduction experiments, the polymer is uniformly distributed across the pipe (i.e., a homogeneous solution). In the present work, injection followed by diffusion implies a nonuniform polymer concentration $C = C(x, r)$ in the pipe flow. Defining a mean concentration C_{av} to be average of $C(x, r)$ over the cross-sectional area of the pipe, we have

$$C(x, r) = C_p \text{ for } x/d \rightarrow 0 \quad (7)$$

$$C(x, r) = C_{av} \text{ for } x/d \rightarrow \infty \quad (8)$$

The average concentration of the polymer solution was calculated as:

$$C_{av} = \left(\frac{Q_p}{Q_w + Q_p} \right) C_p. \quad (9)$$

As indicated by Eq. 8, the polymer concentration becomes uniform at large distances from the injector and hence we may expect an asymptotic level of drag reduction under these circumstances. This constant drag reduction may be compared to the values obtained with homogeneous solutions and in order to assess the effects of concentration, dependence on Reynolds number and onset shear stress, we made use of some of the well-established empirical correlations. To begin with, the concentration depen-

dence can be expressed in universal form (Little et al., 1975) by

$$\frac{C}{DR} = \frac{\{C\}}{DR_m} + \frac{C}{DR_m} \quad (10)$$

where the intrinsic concentration is defined by

$$\{C\} = DR_m / \lim_{C \rightarrow 0} (DR/C). \quad (11)$$

Also the Prandtl-Von Karman law,

$$f^{-1/2} = 4.0 \log_{10}(Re f^{1/2}) - 0.4, \quad (12)$$

may be generalized to polymer solutions (Virk, 1975) in the form:

$$f^{-1/2} = (4.0 + \delta) \log_{10}(Re f^{1/2}) - (0.4 + \delta \log_{10}(\sqrt{2}dW^*)), \quad (13)$$

where δ is the slope increment parameter and W^* may be expressed in terms of the friction velocity at onset of drag reduction, thus:

$$W^* = u_{CR}^* / \nu. \quad (14)$$

Preparation of Drag-Reducing Solutions

We used two different kinds of polymer. One was a polyacrylamide manufactured by Dow Chemicals under the trade name Separan AP30 and had a molecular weight of 3×10^6 (as estimated by the manufacturer). This polymer is an effective drag-reducer in turbulent shear flows and forms a weakly anionic solution. The other was a polyethyleneoxide manufactured by Union Carbide under the trade name Polyox WSR 301. It has a molecular weight of 5×10^6 (as estimated by the supplier) and forms nonionic solutions.

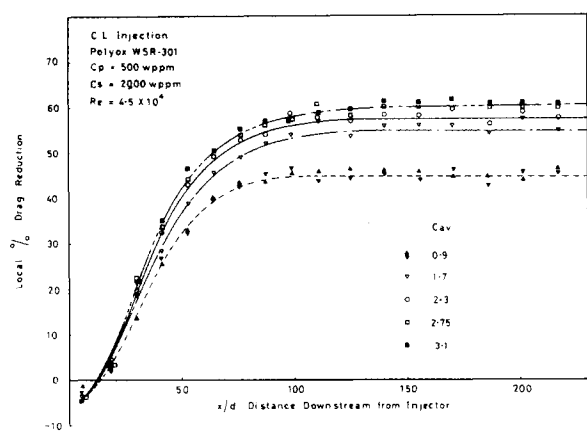
To prepare the solutions, the polymer (as supplied, in powder form) was sprinkled on the surface of the water, which already contained dissolved salt. After gently stirring, solution homogeneity was checked by eye, and the solutions were used within two or three days to minimize any effects due to solution age.

RESULTS AND DISCUSSION

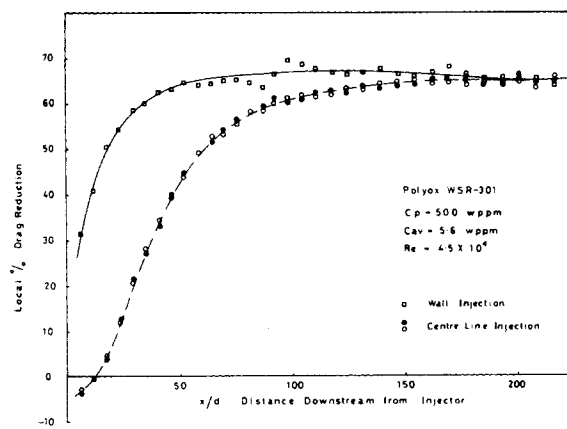
Careful preliminary tests were made with water flow only, in order to check the hydraulic performance of the apparatus and ensure that the measurement systems gave accurate results. In particular, we verified that: the flow in the test section was well-developed; the friction factor was related to the Reynolds number by the Prandtl-Von Karman law; the diffusion of injected salt solutions was in agreement with the results of other workers; and the injection of plain water had no effect on the local friction factor at any value of x/d . These results are not presented here (although some will be given for purposes of comparison in the following sections), but a full account will be found in the thesis by Rabie (1978).

Results were then obtained for the centerline injection of Separan AP30 ($Re = 3.6 \times 10^4$; salt concentration, $C_s = 2,500$ wppm) at master solution concentrations of $C_p = 1,000, 2,000$ and $3,000$ wppm; and for Polyox WSR 301 ($Re = 4.5 \times 10^4$; $C_s = 2,000$ wppm) at $C_p = 500, 1,000, 3,000$ and $5,000$ wppm. Some results were also obtained for Polyox WSR 301 at $C_p = 1,000$ wppm over a range of Reynolds numbers. Injection at the wall was restricted to Polyox WSR 301 ($Re = 4.5 \times 10^4$; $C_s = 2,000$ wppm) at $C_p = 500, 1,000$ and $3,000$ wppm. In every case, experiments were carried out for a range of injection flow rates so that the asymptotic final concentration of polymer in the water flow (i.e., C_{av}) was also varied.

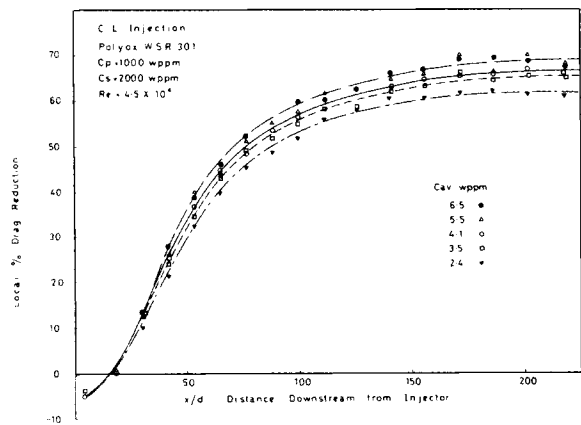
The results for wall injection were restricted partly for expediency—we wished to have enough time to make the LDA measurements to be reported in Part II—and partly because of certain technical problems, which are discussed in the next section. The full set of results may be found in the thesis by Rabie (1978). In the following sections we present a representative sample.



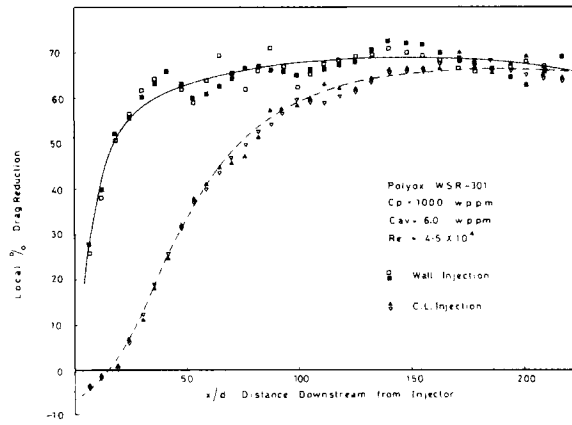
(a) $C_p = 500$ wppm



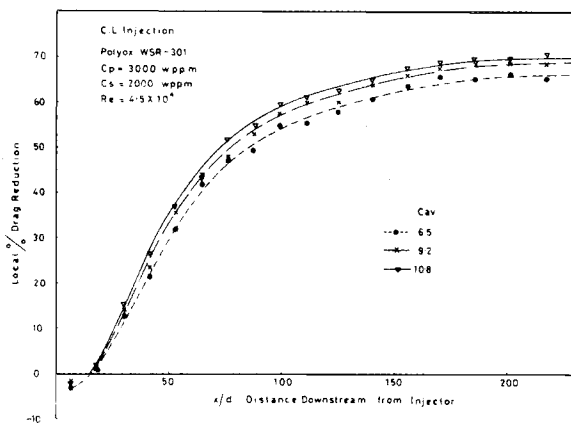
(a) $C_p = 500$ wppm



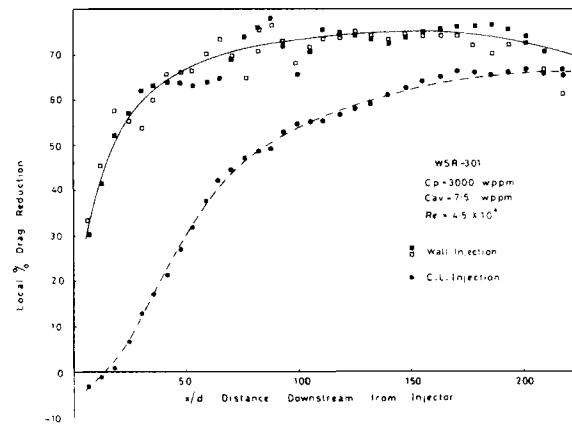
(b) $C_p = 1,000$ wppm



(b) $C_p = 1,000$ wppm



(c) $C_p = 3,000$ wppm



(c) $C_p = 3,000$ wppm

Figure 2. Variation of local drag reduction with downstream distance after injection of Polyox WSR 301 at the centerline.

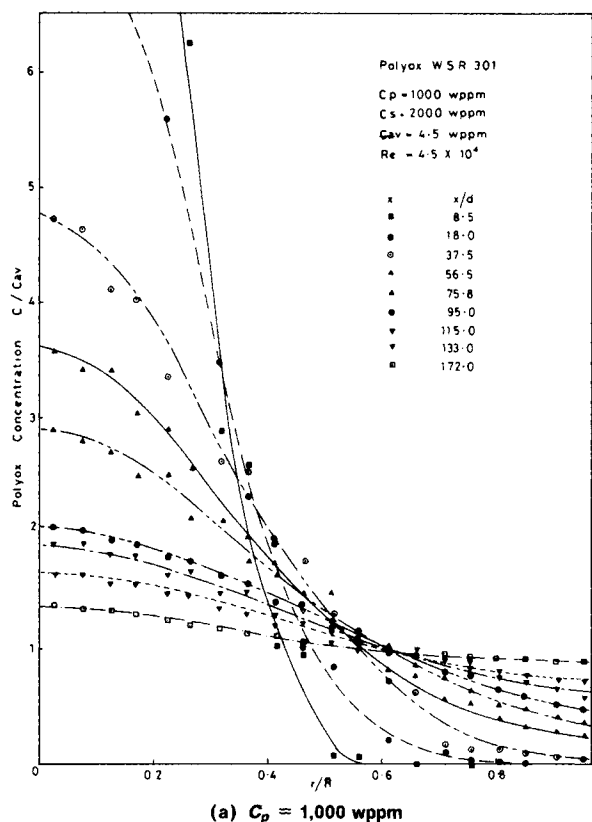
Figure 3. Variation of local drag reduction with downstream distance after injection of Polyox WSR 301 at the wall.

Local Drag Reduction and Polymer Concentration Profiles

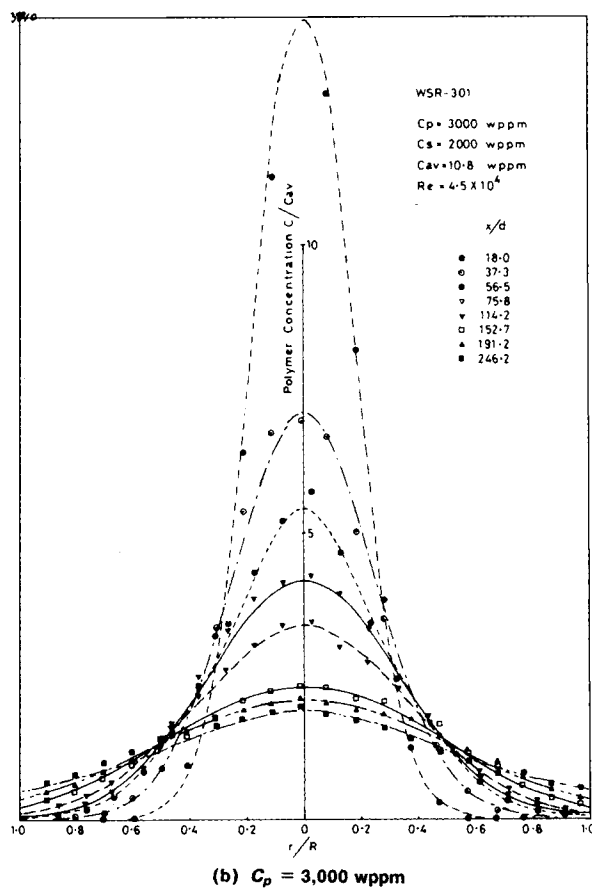
Results for local drag reduction as a function of x/d (Polyox at $C_p = 500, 1,000$ and $3,000$ wppm) are shown for centerline injection in Figures 2(a-c) and for wall injection in Figures 3(a-c). The general feature of the Figures 2(a-c) is the smooth build-up of drag reduction from a small negative value just downstream from the injector, to a substantial asymptotic value some distance downstream. The straight-forward interpretation of these results is that the drag reduction increases as the polymer spreads out radially. The slight drag increase at small x/d is not due to the injection process as such, but must depend on the nature of the polymer solutions. This is borne out by an observed dependence on C_p , but not on injection flow rate. Such initial drag increases have previously been reported by Wells and Spangler (1967) and Maus and Wilhelm (1970).

When we turn to the results for wall injection, the most obvious difference, is the relatively rapid development of local drag reduction with x/d . This difference was found to increase with increasing values of C_p . Two other differences are worthy of note. First, there is the scatter of the data points following injection at the wall. This will be dealt with separately in a later section. Second, if we ignore this scatter and concentrate on the mean of the data points, it is evident that there is an "overshoot." That is, the drag reduction rises to a peak value and then declines with increasing x/d to the same asymptotic level as for centerline injection.

In all, these results seem to suggest that the polymer molecules are effective *near* the wall but not *at* the wall. The overshoot is presumably due to a corresponding overshoot of polymer concentration in an effective annulus near the wall. As the polymer from the wall slot spreads on out radially into the bulk flow, the



(a) $C_p = 1,000$ wppm

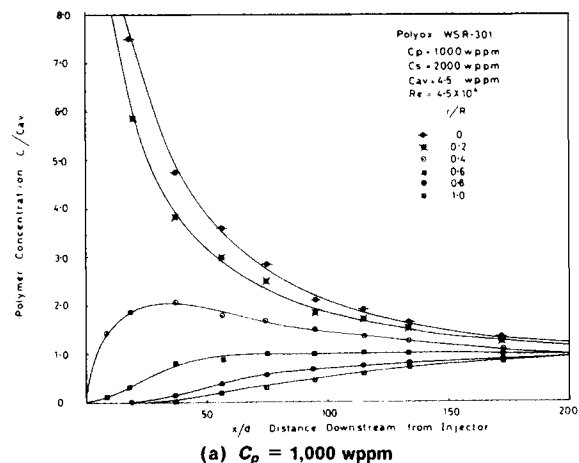


(b) $C_p = 3,000$ wppm

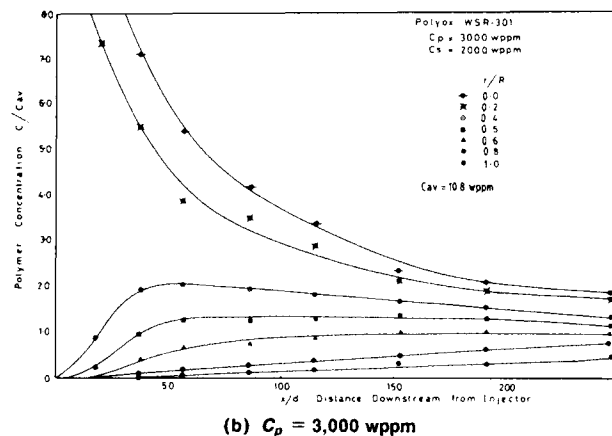
Figure 4. Polymer radial concentration profiles at various distances downstream after injection of Polyox WSR 30L at the centerline.

concentration in the effective annulus will drop to the uniform, average value.

Strong support for this picture is provided by the measurements



(a) $C_p = 1,000$ wppm



(b) $C_p = 3,000$ wppm

Figure 5. Development of polymer concentration with x/d at various radial positions after injection of Polyox WSR 301 at the centerline.

of polymer concentration after injection at the centerline. Concentration profiles are presented for Polyox WSR 301 at $C_p = 1,000$ and $3,000$ wppm in Figures 4(a,b), and the spreading out with increasing x/d may be clearly seen. Interestingly, even the weakest polymer solution took at least four times as long as the plain salt solution to reach complete uniformity, thus the turbulent diffusion process is very much suppressed by the polymer solution. The possibility of relating the streamwise variation of drag reduction to the polymer concentration in an effective annulus may be seen from Figures 5(a,b), where the variation of concentration with x/d is given for various radial positions.

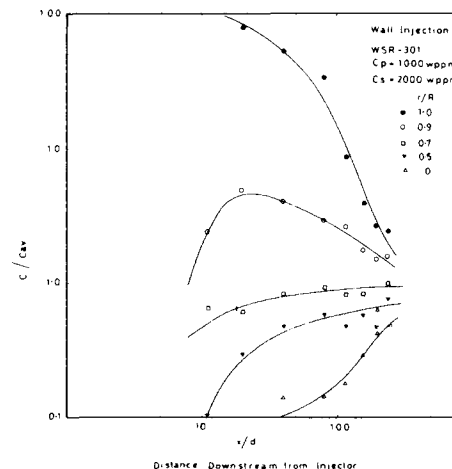
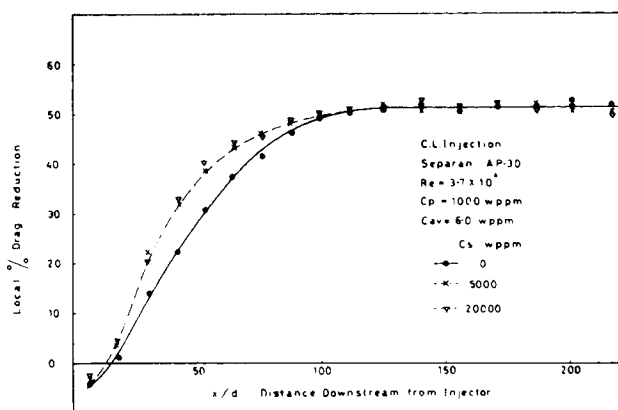
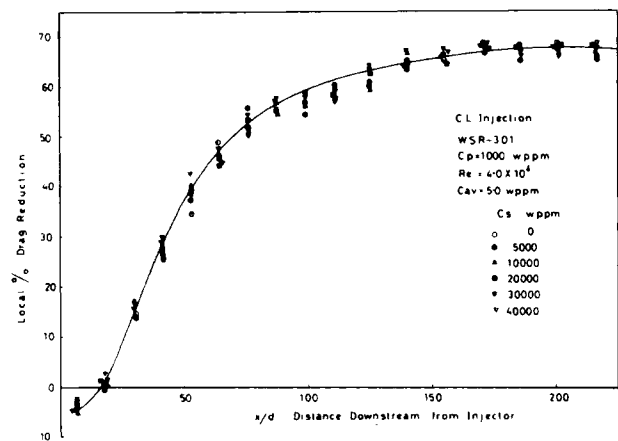


Figure 6. Development of polymer concentration with x/d at various radial positions after injection of Polyox WSR 30L at the wall: $C_p = 1,000$ wppm.

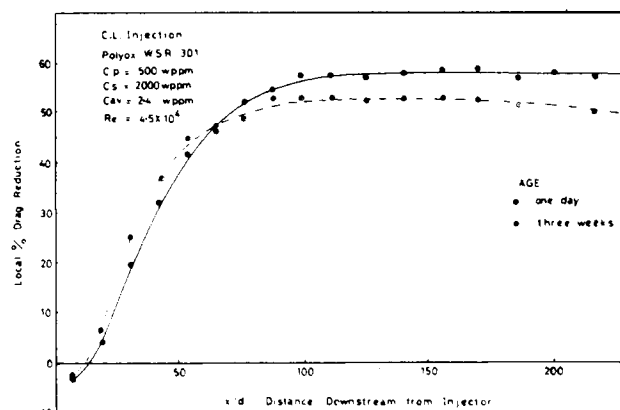


(a) Separan AP 30; $C_p = 1,000$ wppm

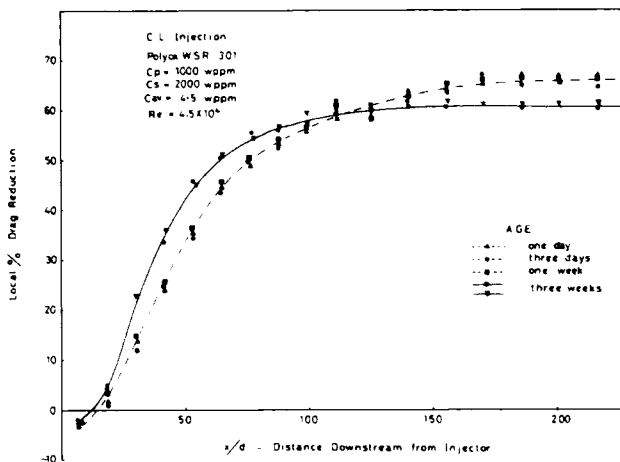


(b) Polyox WSR 301; $C_p = 1,000$ wppm

Figure 7. Effect of NaCl tracer on local drag reduction after injection at the centerline.



(a) $C_p = 500$ wppm



(b) $C_p = 1,000$ wppm

Figure 8. Effect of solution age on local drag reduction after injection of Polyox WSR 301 at the centerline.

When the polymer solutions are injected at the wall, there are difficulties in the way of obtaining a quantitative relation between drag reduction and local polymer concentration. The scatter in the drag reduction curves, along with the rapid development of the relevant variables from the injection point, both pose a severe test of the accuracy of the sampling measurements. For this reason (and the expedient factor, mentioned earlier), we made only one set of diffusion measurements for $C_p = 1,000$ wppm in order to demonstrate the diffusion of the polymer from the wall and permit some rather qualitative comparisons.

Effects of Dissolved Salt and Solution Age

Here, we consider two aspects of solution preparation which might affect our results. First, there is the salt used as a tracer. Early tests indicated that asymptotic drag reduction was not affected by the presence or absence of salt. The effect on the development of local drag reduction was also tested and the results for both polymers are shown in Figures 7(a,b). Clearly, there is a faster development with x/d for Separan in the presence of salt. However, the effect did not depend on C_s in the range tested and the asymptotic drag reduction was unaffected. In the case of Polyox, no effect was observed due to salt.

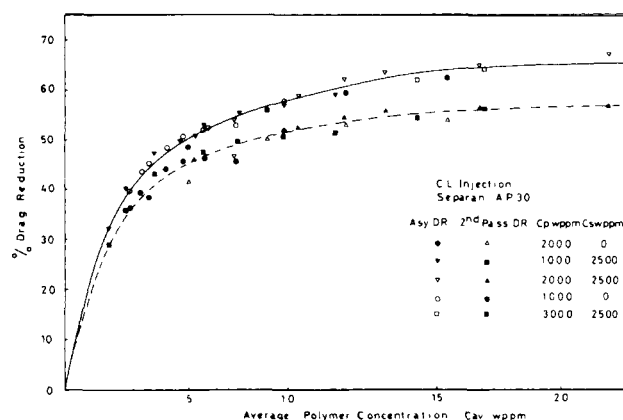
At this point, we should also consider the validity of using salt as a tracer (i.e., the assumption that relative concentration of polymer = relative concentration of salt). A full discussion of this point, based on calculated molecular and turbulent Schmidt numbers for polymer and salt solutions, has been given by Rabie (1978), who concluded (like other investigators) that NaCl is a good tracer for polymer solutions. We shall not reproduce this here but merely note that the results so far, and the analysis presented in the following sections, support this view. Thus, in particular we would

mention the following points: the diffusion measured by salt in polymer solutions is much reduced compared to plain salt solutions; the relationships found here between drag reduction and polymer concentration are physically sensible and internally self-consistent; and these relationships are the same for both types of polymer and the drag reduction asymptotes, as the measured polymer concentration becomes uniform.

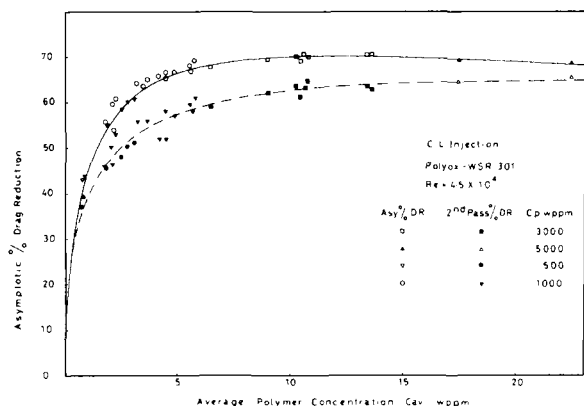
The effect of ageing the polymer solutions was investigated by storing solutions for various periods after they had been mixed. Typical results are presented in Figures 8(a,b) for Polyox WSR 301 at $C_p = 500$ and 1,000 wppm. No significant effect was found for solutions up to about one week old. Older solutions showed a more rapid streamwise development of local drag reduction, but the asymptotic value was reduced compared to fresh solutions.

Peak (or Asymptotic) Drag Reduction

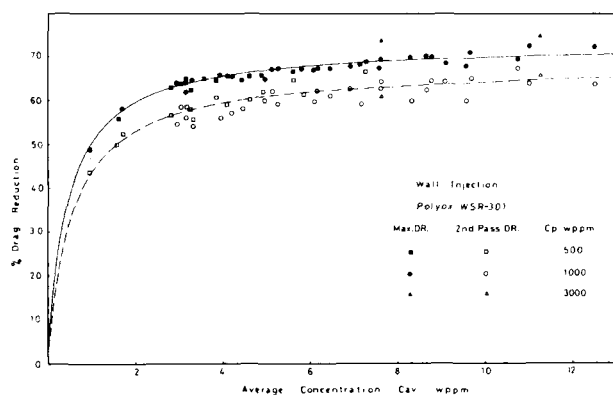
In Figures 9(a) and 9(b), the asymptotic drag reduction in the first pass is compared to the homogeneous drag reduction in the second pass, for Separan and Polyox respectively, after injection at the centerline. The magnitude of drag reduction in the second pass is somewhat smaller than the asymptotic value in the first pass. This might be due to degradation (i.e., molecular scission due to shear); but this seems unlikely, as the difference is greater in Separan, which is well known to be more resistant than Polyox to degradation. Figure 9(c) shows the corresponding plot of peak drag reduction in the first pass and homogeneous drag reduction in the second pass for injection of Polyox at the wall. Evidently, the difference between first- and second-pass values is smaller than in the centerline case, presumably reflecting the shorter time spent subject to turbulent shear when injection is at the wall. Like the results for solution ageing, discussed in the previous section, we think the most



(a) Separan AP 30: injection at the centerline.



(b) Polyox WSR 301: injection at the centerline.



(c) Polyox WSR 301: injection at the wall.

Figure 9. Peak drag reduction against average polymer concentration.

likely explanation of these differences is in terms of the break-up supermolecular aggregates. We shall return to this point shortly.

In Figure 10, we show the effect of varying Reynolds number at various values of C_{av} . Here, the friction factor is based on the asymptotic value for the first pass when Polyox is injected at the centerline (for the case $C_p = 1,000$ wppm). It is clear that, like the well known results for homogeneous drag reduction, the experimental results are bounded by two extremes: the agreement of the results for water with the Prandtl-Von Karman law on the one hand, and the maximum drag reduction asymptote of Virk, on the other.

A significant feature of our present results is the large magnitudes of the asymptotic drag reduction, compared to values obtained in homogeneous drag reduction under comparable conditions. This effect has previously been reported by Vlegaar and Tels (1973), who also noted that the difference was greater at low Reynolds

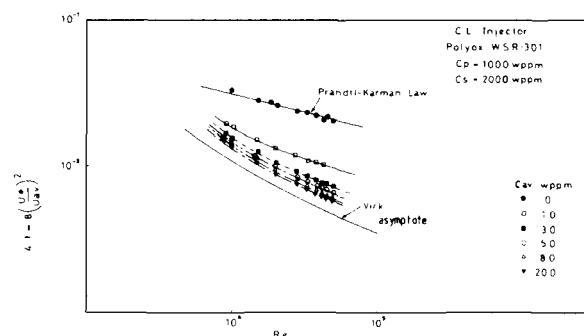


Figure 10. Friction factor against Reynolds number for Polyox WSR 301 injected at the centerline.

numbers. To assess the dependence on average polymer concentration, and also make a comparison with the results of other investigations, we plotted C_{av}/DR against C_{av} for our results. As may be seen in the thesis by Rabie (1978), all results fitted the straight line predicted by Eq. 10 rather well. Using Eqs. 10 and 11, values of $\{C\}$, DR_m and $DR_m/\{C\}$ were calculated for each set of results. These values are presented in Table 1, where they may be compared with the results of other investigations. In particular, we note the smaller effect found by Vlegaar and Tels (1973). This may be attributed to their pressure taps being positioned where (according to our results) the drag reduction effect was still developing.

The dependence on Reynolds number and the onset effect were investigated for the one case of Polyox at $C_p = 1,000$ wppm, injected at the centerline. These results were plotted in Prandtl-Von Karman coordinates for a range of values of C_{ac} (Rabie, 1978). The onset point was found to correspond to a Reynolds number of 2.3×10^3 , indicating that drag reduction was present from about the beginning of the turbulent regime. Using Eqs. 13 and 14 to fit this data, a comparison of our values of the onset wall shear stress and slope increment factor with representative results from other investigations is given in Table 2.

The large drag reduction (along with ageing effects and differences between first and second pass, and between centerline and wall injection) is probably due to a degree of inhomogeneity in the injection process in that polymer may reach the critical region near the wall in the form of aggregates rather than as individual molecules. Such agglomerations of polymer molecules are known to be present in solutions and to be more effective than single molecules in reducing drag (Cox et al., 1974; Dunlop and Cox, 1977). Also aggregates of this kind may be expected to interact with a wider range of eddy sizes than individual molecules, hence reducing the wall shear stress at onset.

Relationship between Local Drag Reduction and Spatial Distribution of Polymer

The qualitative explanation of the observed streamwise variation in local drag reduction seems clear. As the injected polymer travels downstream, it spreads out radially. The polymer concentration in (loosely) the "wall region" therefore increases with x/d and hence the local drag reduction also increases. Ultimately, when the polymer is uniformly spread across the pipe, the drag reduction reaches its asymptotic value.

Let us assume that drag reduction is determined by polymer concentration in an annulus with inner and outer radii r_1 and r_2 , respectively. Then we may characterize the annulus by its centroid coordinate

$$r_m = \frac{r_1 + r_2}{2} \quad (15)$$

and its thickness

$$\Delta r = r_2 - r_1. \quad (16)$$

In the present work, the concentration depends on position so we

TABLE 1. VALUES CALCULATED USING EQS. 10 AND 11

Polymer	$M \times 10^{-6}$	Solution	$\{C\}$ wppm	%DR _m	%DR _m / $\{C\}$	Reference
Seyaran AP30*	3.0	Homogeneous	4.0	36.0	9	Whittsitt et al. ¹ (1968)
	3.0	C.L. Injection	3.0	50	16.7	Vleggaar & Tels (1973)
	3.0	Asymptotic	2.0	69.0	34.5	} Present Work
		Second Pass	2.1	63.0	30.0	
Polyox WSR-301**	5.3	Homogeneous	1.5	58.0	39.0	Virk (1975)
	4.5	Homogeneous	1.25	60.0	43.0	McNally ² (1968)
	5	Asymptotic	0.65	72.5	111.5	} Present Work
	5	Second Pass	0.95	68	71.5	
	5	Maximum DR ⁺	0.50	74	148	} C.L. Injection
	5	Second Pass ⁺	0.65	68	105	
	5	Maximum D.R. ⁺⁺	0.30	76.5	255	
	5	Second Pass ⁺⁺	0.70	69.5	99	} Wall Injection

* Seyaran results are at $Re = 3.7 \times 10^4$, except those of Vleggaar & Tels which were at $Re = 5.25 \times 10^4$.

** Polyox WSR-301 results all at $Re = 4.5 \times 10^4$.

⁺ Results of the wall injection $C_p = 500$ and 1,000 wppm.

⁺⁺ Results of the wall injection $C_p = 3,000$ wppm.

¹ Data taken from Wells (1969).

² Data taken from Virk (1975).

TABLE 2. EXPERIMENTAL DATA FOR ONSET WALL SHEAR STRESS AND SLOPE INCREMENT FOR POLYOX WSR-301.

$M \times 10^{-6}$	d cm	C range wppm		τ_w^* N/m ²	$\delta/C^{1/2}$	Reference
3.7	0.27	30		2.9	2.92	Liaw (1968) ⁺
4.7	0.22	0.29–2.2	<i>H</i>		7.8 ± 0.2	Shin (1965) ⁺
5	5.08	2–50	<i>H</i>	0.27 ± 0.05	5.0 ± 4.0	Goren & Norbury (1967)
4.5	2.0	2–40	<i>H</i>	0.45	4.7 ± 0.2	McNally (1968) ⁺
5.3	0.45	1–30	<i>H</i>	—	3.9 ± 0.5	} Virk (1966–1971) ⁺
5.3	0.95	1–30	<i>H</i>	0.7 ± 0.15	4.7 ± 0.2	
5.5	0.85	10–100	<i>H</i>	0.71 ± 0.15	4.6 ± 0.3	
6.1	6.42	20–500	<i>H</i>	0.35 ± 0.1	3.3 ± 0.7	
5	0.78	50	<i>I</i>	0.28 ± 0.02	2.2 ± 0.5	} Stenberg et al. (1977a)
5	1.03	10–50	<i>I</i>	0.25 ± 0.05	3.8 ± 1.0	
4	4.13	3–9	<i>W</i>	0.2 ± 0.05	2.2 ± 0.2	Maus & Wilhelm (1970)
4	30.5	2–6	<i>W</i>	0.13 ± 0.02	6.5 ± 0.5	Ramu & Tullis (1976)
5	2.6	1–20	<i>CL</i>	0.064 ± 0.005	6.1 ± 1.2	Present Work

W = wall injection results

CL = centerline injection results

I = other injection methods

H = results of homogeneous polymer solutions

⁺ = data taken from Virk (1975)

use the concentration averaged over the annulus cross-section, thus:

$$\bar{C}(x, r_m) = \frac{1}{r_m \Delta r} \int_{r_m - \Delta r/2}^{r_m + \Delta r/2} C(x, r) dr. \quad (17)$$

Provided we choose the correct values for r_m and Δr , it seems a reasonable inference that local drag reduction will be determined by $\bar{C}(x, r_m)$. It is also reasonable to infer that the magnitude of this local drag reduction will be equal to what would be measured in

a flow with a uniform polymer concentration equal to the particular value of \bar{C} (i.e., a flow in which $C(x, r) = C_{av} = \bar{C}$). Thus, for a given \bar{C} , the predictions of local drag reduction was obtained from Figure 9(a) for Seyaran and Figure 9(b) for Polyox.

As the first stage in our analysis, we took $\Delta r = 0$ and varied the annular position from $r_m/R = 1.0$ to 0.75, in steps of 0.05. Next, we took $\Delta r = 0.05R$ and repeated the process. The results for Polyox WSR 301 ($C_p = 1,000$ wppm, $C_{av} = 4.5$ wppm) for these two values of Δr are shown in Figure 11 and 12. In both cases, there

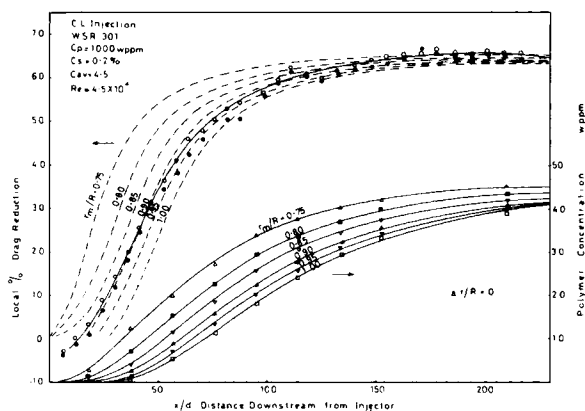


Figure 11. Prediction of variation in drag reduction with x/d , from the streamwise variation of polymer concentration: effective annular thickness $\Delta r = 0$.

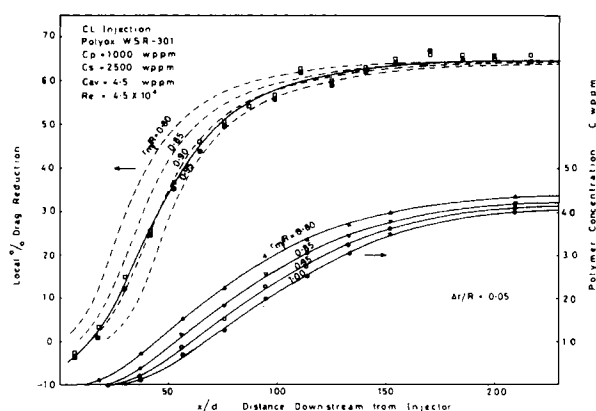
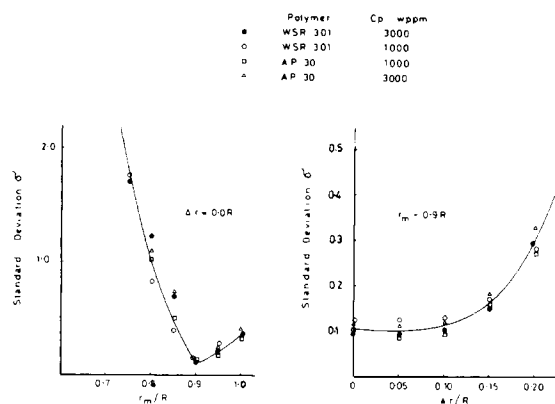


Figure 12. Prediction of variation in drag reduction with x/d , from the streamwise variation of polymer concentration: effective annular thickness $\Delta r = 0.05 R$.



(a) Variation of standard deviation with centroid radius r_m

(for $\Delta r = 0$).

(b) Variation of standard deviation with annular thickness

Δr (for $r_m = 0.9 R$).

Figure 13. Effect of varying effective annulus parameters, r_m and Δr , on the prediction of streamwise variation of drag reduction.

is good agreement between the predicted local drag reduction of the annulus with $r_m = 0.9R$ and the experimental values. The thickness of the annulus was further increased to $0.1R$, $0.15R$ and $0.20R$ and the analysis repeated. In all cases, the best fit was obtained with $r_m = 0.9R$.

The analysis was tested by calculating the standard deviation of the data points from the predicted curve for each value of r_m and Δr . The results for both polymers and for injection concentrations $C_p = 1,000$ and $3,000$ wppm are presented in Figures 13 (a,b). From these graphs, we may tentatively conclude that the polymer molecules (or aggregates) exert their main effect on the flow within an annulus centered at $r_m = 0.9R$ and with a thickness of about $0.1R$ in our particular flow conditions. To put this in more universal form, it corresponds to dimensionless distances from the wall $15 \leq y^+ \leq 100$, where y^+ is calculated from asymptotic values of U^* and V taken at large x/d . These bounds agree with the values deduced by Virk (1975) from indirect evidence.

Quasi-Cyclic Variations during Injection at Wall

The scatter in the results for injection at the wall has already been remarked upon. At first, this scatter was thought to be random. However, after inspection of many sets of data, it seemed clear that this was a fairly regular variation and that its magnitude was larger than any experimental error encountered during this investigation. Good examples of this oscillation are shown in Figure 14, where the continuous curves have now been fitted to the oscillation of the data points rather than to the mean, as previously.

We considered two possible explanations of this behavior. First, there might have been some structural instability in the injection flow, due to the non-Newtonian nature of the fluid being injected (e.g., Vleggaar and Tels, 1973). However, our injection pump was designed to eliminate this effect and tests indicated that the effect of structural (or other) instability in the injection process was negligible.

Second, the well-known turbulent bursting process could be modulating the outward diffusion of polymers from the wall. Such a quasi-cyclic process (as defined by Offen and Kline, 1975) will presumably impose a periodicity on the transfer of polymer solution from the wall to the buffer region. Thus, a wave-like variation of concentration in the buffer region due to the bursting process seems a plausible explanation of the oscillatory behavior in Figure 14.

If this is indeed the case, the periodicity of the curves in Figure 14 should be related to the mean time between bursts. Let us con-

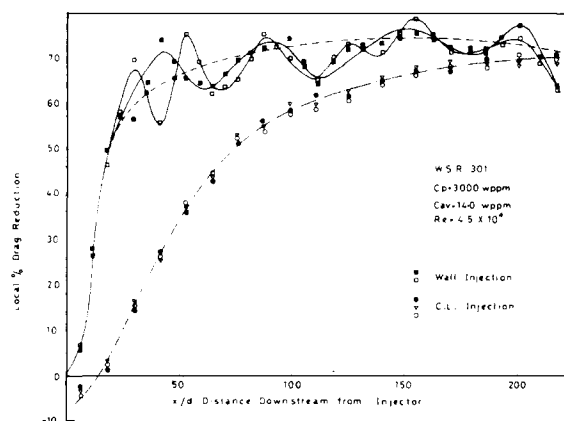


Figure 14. Variation of local drag reduction with x/d , after injection of Polyox WSR 301 at the wall, showing quasi-cyclic variations.

sider, therefore, the oscillatory part of the drag reduction curves and let L_x be the distance between any two successive crests. Evidently, for any fixed set of experimental conditions, L_x is a random variable. Taking its ensemble average, the mean time between bursts should be:

$$T_B = \langle L_x \rangle / U_B \quad (18)$$

where U_B is the streamwise mean velocity of the large-scale burst structures. We evaluated $\langle L_x \rangle$ from three or four cycles of each pressure curve (as in Figure 14) and from seven such curves in all. U_B was taken to be $0.8 U_o$ (e.g., Offen and Kline, 1975). The result was

$$T_B = \langle L_x \rangle / U_B = 0.41 \pm 0.06 \text{ s} \quad (19)$$

To check this, we used the LDA to measure the autocorrelation of the streamwise fluctuating velocity $R_{11}(\tau)$. Individual (i.e., single realization) values of T_B were obtained from the first cycle of the $R_{11}(\tau)$ curve, as we shall discuss in Part II. Then, 49 such curves were used to form an ensemble average, with the result:

$$T_B = 0.43 \pm 0.05 \text{ s} \quad (20)$$

The agreement between these two values of T_B suggests that our explanation of the oscillations in the drag reduction graphs deserves to be taken seriously. However, it should still be regarded as rather tentative, until some more direct evidence (possibly using flow visualization) is forthcoming.

NOTATION

$\langle \rangle$	= ensemble average
$C, C(x, r)$	= polymer concentrations; uniform, nonuniform,
C_{av}, C_p, C_o	bulk mean, master solution, intrinsic, wppm
$\{C\}$	
C_s	= salt (NaCl) concentration, wppm
dp/dx	= streamwise pressure gradient
d	= pipe diameter
DR, DR_m	= drag reduction, maximum drag reduction, %
f	= friction factor
Q_p	= injection volumetric flow rate of master solution
Q_w	= volumetric flow rate of water in the pipe
r	= radial coordinate
r_1, r_2, r_m	= inner, outer and centroid radii of effective annulus
R	= pipe radius
Re	= Reynolds number, $(= \bar{U}_{av} d / \nu)$
$R_{11}(\tau)$	= autocorrelation of streamwise fluctuating velocity
T_B	= mean time between bursts

U^*, U_{cr}^* = friction velocity; friction velocity at onset of drag reduction
 \bar{U}_{ao}, U_0, U_B = mean velocities; bulk mean, centerline, of burst structures
 W^* = parameter in Eq. 13 ($= U_{cr}^*/\nu$)
 x = downstream distance ($x = 0$ at point of injection)
 $y, y+$ = distance from wall ($y+ = yu^*/\nu$)

Greek Letters

δ = slope increment parameter in Eq. 13
 ΔP_p = pressure drop after polymer injection
 ΔP_w = pressure drop before polymer injection
 Δr = radial thickness of effective annulus
 ν = kinematic viscosity
 ρ = density
 σ = standard deviation of data points from predicted curves of local DR against x/d
 τ = delay time in autocorrelation
 τ_w = wall shear stress
 τ_w^* = wall shear stress at onset of drag reduction

LITERATURE CITED

- Cox, L. R., A. M. North, and E. H. Dunlop, "Evidence for a Time-Scale Effect in Drag Reduction in Solutions of Polystyrene in Toluene," Proc. 1st Int. Conf. on Drag Reduction, Cambridge, UK (BHRA: 1974).
- Dunlop, E. H., and L. R. Cox, "Influence of Molecular Aggregates on Drag Reduction," *Phys. Fluids*, **20**, S203 (1977).
- Goren, Y., and J. F. Norbury, "Turbulent Flow of Dilute Aqueous Polymer Solutions," *Trans. ASME: J. Basic Eng.*, **89**, 814 (1967).
- Granville, P. S., "Drag Reduction of Flat Plates with Slot Ejection of Polymer Solutions," NSRDC Report 3158 (1969).
- Hoyt, J. W., "The Effect of Additives on Fluid Friction," *Trans. ASME: J. Basic Engineering*, **94**, 258 (1972).
- Hoyt, J. W., "Polymer Drag Reduction—a Literature Review, 1975–76," Paper A1: Proc. 2nd Int. Conf. on Drag Reduction, Cambridge, UK (BHRA: 1977).
- Johnson, B., and R. H. Barchi, "Effect of Drag-Reducing Additives on Boundary-Layer Turbulence," *J. Hydronautics*, **2**, 168 (1968).
- Kowalski, T., and E. Brundrett, "Macromolecular Entanglement Hypothesis in Drag Reduction Flows," Paper C1: Proc. 1st Int. Conf. on Drag Reduction, Cambridge, UK (BHRA: 1974).
- Latto, B., and C. H. Shen, "Effect of Dilute Polymer Solution Injection on External Boundary Layer Phenomena" *Can. J. Chem. Eng.*, **48**, 34 (1970).
- Little, R. C., R. J. Hansen, D. L. Hunston, O. K. Kuri, R. L. Patterson and R. Y. Ting, "The Drag Reduction Phenomenon," *Ind. Eng. Chem. Fund.*, **14**, 283 (1975).
- Love, R. H., "The Effect of Ejected Polymer Solutions on the Resistance and Wake of a Flat Plate in a Water Flow," *Hydronautics Inc. Tech. Report* 353 (1965).
- Maus, J. R., and L. R. Wilhelm, "Effect of Polymer Injection on Frictional Drag in Turbulent Pipe Flow," *J. Hydronautics*, **4**, 35 (1970).
- McComb, W. D., and L. H. Rabie, "Drag-Reducing Polymers and Turbulent Bursts," *Nature*, **273**, 653 (1978).
- McComb, W. D., and L. H. Rabie, "Development of Local Turbulent Drag Reduction due to Nonuniform Polymer Concentration," *Phys. Fluids*, **22**, 183 (1979).
- McComb, W. D., and K. T. J. Chan, "Drag Reduction in Fibre Suspensions: Transitional Behaviour due to Fibre Degradation," *Nature*, **280**, 45 (1979).
- McComb, W. D., and S. Ayyash, "The Production, Pulsation and Damping of Small Air Bubbles in Dilute Polymer Solutions," *J. Phys. D.: Appl. Phys.*, **13**, 773 (1980).
- Offen, G. R., and S. J. Kline, "A Proposed Model of the Bursting Process in Turbulent Boundary Layers," *J. Fluid Mech.*, **70**, 209 (1970).
- Rabie, L. H., "Drag Reduction in Turbulent Shear Flow due to Injected Polymer Solutions," Ph.D. Thesis, Edinburgh University (1978).
- Ramu, K. L., and J. P. Tullis, "Drag Reduction in Developing Pipe Flow with Polymer Injection," Paper G3: Proc. 1st Int. Conf. on Drag Reduction, Cambridge, UK (BHRA: 1974).
- Ramu, K. L., and J. P. Tullis, "Drag Reduction and Velocity Distribution in Developing Pipe Flow," *J. Hydronautics*, **10**, 55 (1976).
- Stenberg, L.-G., T. Lagerstedt, O. Sahlen, and E. R. Lindgren, "Mechanical Mixing of Polymer Additives in Turbulent Drag Reduction," *Phys. Fluids*, **20**, 858 (1977a).
- Stenberg, L.-G., T. Lagerstedt, and E. R. Lindgren, "Polymer Additive Mixing and Turbulent Drag Reduction," *Phys. Fluids*, **20**, S276 (1977b).
- Virk, P. S., "Drag Reduction Fundamentals," *AIChE J.*, **21**, 625 (1975).
- Walters, R. R., and C. S. Wells, "An Experimental Study of Turbulent Diffusion of Drag-Reducing Polymer Additives," *J. Hydronautics*, **5**, 65 (1971).
- Wells, C. S., ed., *Viscous Drag Reduction*, Plenum Press (1969).
- Wells, C. S., and J. G. Spangler, "Injection of Drag-Reducing Fluid into Turbulent Pipe Flow of a Newtonian Fluid," *Phys. Fluids*, **10**, 1890 (1967).
- Wu, J., "Some Techniques of Ejecting Additive Solutions for Drag Reduction," *Hydronautics Inc. Technical Report* 7101-1 (1971).
- Vleggaar, J., and M. Tels, "Drag reduction by polymer threads," *Chem. Eng. Sci.*, **28**, 965 (1973).

Manuscript received April 6, and accepted October 13, 1981